

# The Role of Soil Moisture and Surface and Subsurface Water Flows on Predictability of Convection



J. Arnault and H. Kunstmann

**Abstract** Since June 2018 we have further assessed the mechanism through which a more sophisticated treatment of terrestrial hydrological processes in a numerical weather prediction model potentially improves the predictability of convection. In order to achieve this, we have implemented the so-called soil-vegetation-atmospheric water tagging procedure in WRF and WRF-Hydro (Skamarock and Klemp in *J Comp Phys* 227:3465–3485, 2008 [3]; Gochis et al. in *The WRF-Hydro model technical description and user’s guide*, version 3.0, NCAR Technical Document :120, 2015 [2]). This tagging procedure is used to track a source of water through the terrestrial and atmospheric water compartments in the model. The tagging enhanced versions of WRF and WRF-Hydro are named WRF-tag and WRF-Hydro-tag. A publication detailing the implementation of WRF-tag and WRF-Hydro-tag with an application case-study has been recently published in *Water Resources Research* (Arnault et al. in *Water Resour Res* 55:6217–6243 (2019) [1]). In particular, WRF-tag and WRF-Hydro-tag are applied to the case of a precipitation event in the Upper Danube river basin. A comparison between WRF-tag and WRF-Hydro-tag results allows to deduce the role of lateral terrestrial water flow on land-atmospheric water pathways, including precipitation.

## Implementation of WRF-tag and WRF-Hydro-tag at ForHLR2

The development of the WRF-tag and WRF-Hydro-tag models started at ForHLR2 in 2016. However, several issues have been encountered, which involved a lot of debugging and several re-run of the simulations presented in Arnault et al. [1]. The two main improvements which have been considered since June 2018 are:

---

This project is part of the DFG (German Research Foundation) Collaborative Research Center (CRC) 165/1 “Wave to Weather (W2W)”, funded for the period 07/2015–06/2019.

---

J. Arnault (✉) · H. Kunstmann  
Karlsruhe Institute of Technology (KIT), Institute for Meteorology and Climate Research (IMK-IFU), Garmisch-Partenkirchen, Germany  
e-mail: [joel.arnault@kit.edu](mailto:joel.arnault@kit.edu)

© Springer Nature Switzerland AG 2021

W. E. Nagel et al. (eds.), *High Performance Computing in Science and Engineering '19*, [https://doi.org/10.1007/978-3-030-66792-4\\_33](https://doi.org/10.1007/978-3-030-66792-4_33)

493

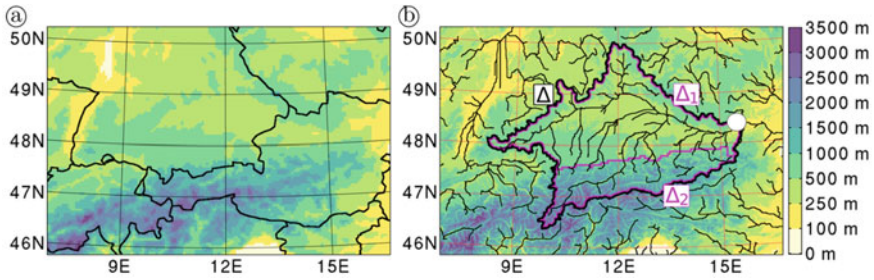


**Fig. 1** **a** Terrain elevation [m a.s.l.] of the 5 km-resolution WRF domain. The solid black lines delineate the political boundaries. **b** Terrain elevation of the routing grid at 500 m resolution coupled with the WRF domain in the WRF-Hydro setup. The thin black lines show river channels with a Strahler stream order equal to or above 5. The bold black contour delineates the part of the upper Danube river basin referred as the study region  $\Delta$ .  $\Delta$  is divided in two subregions delineated by the bold magenta contour:  $\Delta_1$  characterized by moderate topography in the North, and  $\Delta_2$  characterized by steep topography in the South

- Implementation of the double precision for the computation of subrid lateral transport of tagged soil moisture and tagged ponded water, in order to improve the closure of the tagged terrestrial water balance.
- Introduction of a depth-weighting factor equal to the relative amount of tagged liquid soil moisture for the vertical distribution of the tagged lateral subsurface flow, in order to prevent tagged liquid soil moisture in the first soil layer to be directly moved to the bottom soil layer when the tagged liquid soil moisture has not infiltrated to that bottom layer yet.

It is worth to mention here that the access to the ForHLR2 facility contributed to accelerate the development and debugging of WRF-tag and WRF-Hydro-tag. Indeed, the supercomputing environment allowed to test and improve the tagging procedure for a real case, a relatively large simulation domain ( $150 \times 100 \times 50$  grid points), a relatively long simulation period (5 years including 1 year of spinup time), and a relatively short simulation time (about two weeks for the 5 year-simulation). Furthermore, the possibility to process the model output directly at ForHLR2 allowed to quickly diagnose and correct potential bugs in the implementation of the tagging procedure.

### Research highlights obtained with WRF-tag and WRF-Hydro-tag

The newly developed joint soil-vegetation-atmospheric water tagging procedure allows (1) tracking a source of water through the hydrological compartments resolved in WRF-tag and WRF-Hydro-tag, and (2) quantifying the contribution of the WRF-Hydro-resolved lateral terrestrial water flow to the hydrological cycle at regional scale. Arnault et al. ([1], in review) have applied WRF-tag and WRF-Hydro-tag to the case of the upper Danube river basin, using the domain setup displayed in Fig. 1 and a simulation period of 5 years from January 2007 to December 2011.

Arbitrarily, the precipitation event which occurred in the upper Danube river basin between 1200 UTC 14 August 2008 and 1800 UTC 16 August 2008 has been chosen as the source of water for the soil-vegetation-atmospheric water tagging procedure, tagged and tracked for a 40 month-period until December 2011. The tagged results from Arnault et al. ([1], in revision) are analysed in this section with the two following equations, which are the budget of tagged terrestrial water Eq. 1 and the budget of tagged terrestrial water Eq. 2.

$$P^{source} = E^{tagged} + R_{S^{tagged}} + R_G^{tagged} + (S^{tagged})_t \quad (1)$$

$$E^{tagged} = O_{NET^{tagged}} + (W^{tagged})_t + P^{tagged} \quad (2)$$

Equation 1 allows to quantify the partitioning of the source precipitation  $P^{source}$  among the tagged evaporation  $E^{tagged}$ , the tagged surface runoff  $R_{S^{tagged}}$ , the tagged underground runoff  $R_G^{tagged}$ , and the tagged terrestrial water change  $(S^{tagged})_t$ . Equation 2 further allows to quantify the partitioning of  $E^{tagged}$  among the tagged net atmospheric outflow  $O_{NET^{tagged}}$ , the tagged atmospheric water change  $(W^{tagged})_t$  and the tagged precipitation  $P^{tagged}$ .

Figure 2 provides the spatial distribution of tagged water fluxes from Eqs. 1 and 2, accumulated for the whole study period. The left column of Fig. 2 shows the WRF-tag result, whereas the right column shows the differential result between WRF-tag and WRF-Hydro-tag. In WRF-tag,  $P^{source}$  covers the entire study region  $\Delta$ , with lower amounts in the northern subregion  $\Delta_1$  where topography is moderate, and higher amounts in the southern subregion  $\Delta_2$  where topography is steep.  $R_{S^{tagged}}$ ,  $R_G^{tagged}$  and  $E^{tagged}$  display spatial patterns close to those in  $P^{source}$ .  $P^{tagged}$  is comparatively much smaller, with enhanced values in  $\Delta_2$  which suggests that the mountainous part of the basin has a blocking effect on the tagged atmospheric water.

In comparison to WRF-tag, WRF-Hydro-tag generates slightly different spatial patterns of  $P^{source}$ , which directly affect  $E^{tagged}$  and contribute to the small differences in  $P^{tagged}$  (see right column of Fig. 2). The WRF-Hydro-tag induced changes in  $R_{S^{tagged}}$  and  $R_G^{tagged}$  rather follow the differences in topography. In particular, WRF-Hydro-tag generates much more  $R_{S^{tagged}}$  and much less  $R_G^{tagged}$  in  $\Delta_2$ , but slightly less  $R_{S^{tagged}}$  and slightly more  $R_G^{tagged}$  in  $\Delta_1$ . This is related to the more realistic description of the surface runoff generation mechanism in WRF-Hydro, which is more efficient in steep topography gradient areas. Indeed, the subsurface lateral water flow accumulates soil moisture towards valley bottoms. In steep terrain this generates exfiltration, whereas in moderate terrain this accelerates the deep infiltration and increases the underground runoff.

The tagging results are further investigated with time series of accumulated tagged terrestrial water fluxes in Fig. 3 and tagged atmospheric water fluxes in Fig. 4, spatially averaged for the study region  $\Delta$  and the subregions  $\Delta_1$  and  $\Delta_2$ . In comparison to WRF-tag, WRF-Hydro-tag produces less  $R_{S^{tagged}}$  during the tagging event in relation with an increase of the amount of tagged soil moisture storage in both subregions  $\Delta_1$  and  $\Delta_2$ , as shown in Fig. 3. In  $\Delta_1$ , the excess of tagged soil moisture in WRF-Hydro

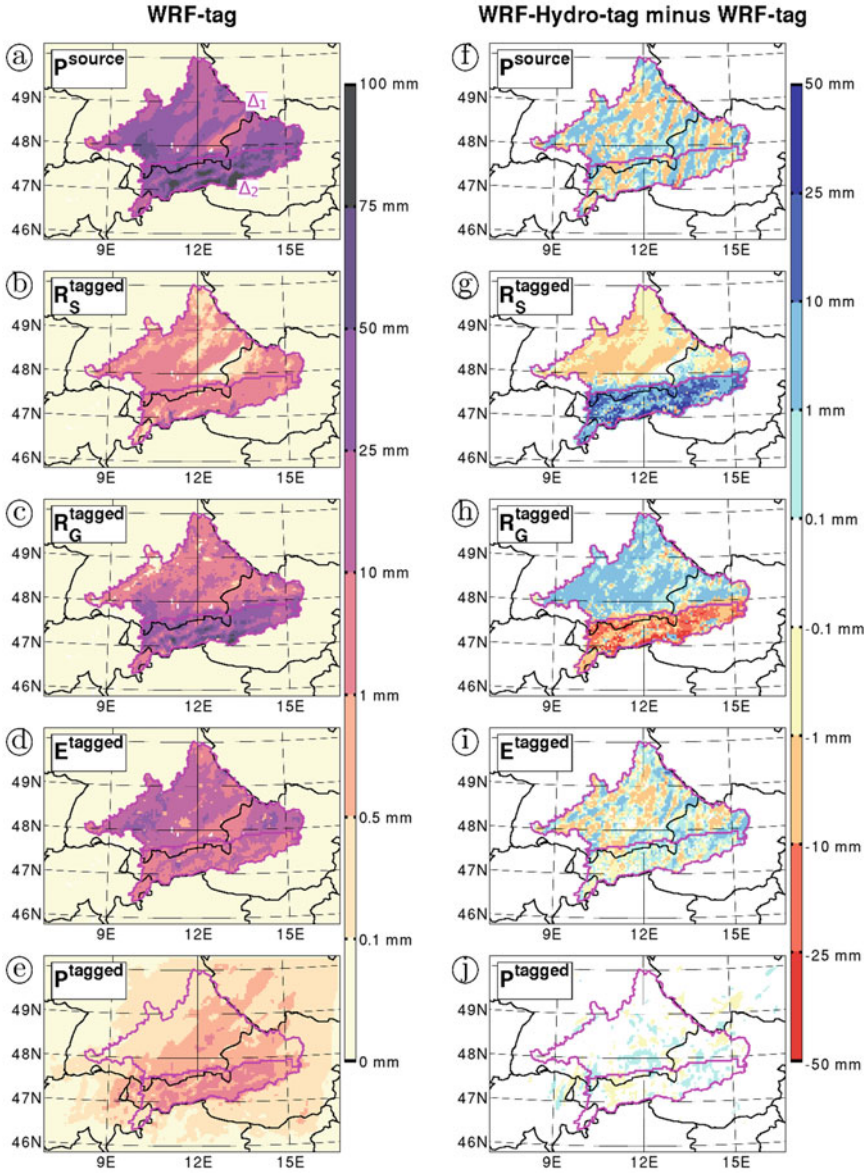


**Fig. 2** a–e Maps of accumulated tagged water fluxes [mm] for the whole study period from 1 January 2008 to 31 December 2011, namely source precipitation  $P^{\text{source}}$ , tagged surface runoff  $R_S^{\text{tagged}}$ , tagged underground runoff  $R_G^{\text{tagged}}$ , tagged surface evaporation  $E^{\text{tagged}}$ , and tagged precipitation  $P^{\text{tagged}}$ , derived from WRF-tag. (f–j) As in (a–e), except for the difference between WRF-Hydro-tag and WRF-tag

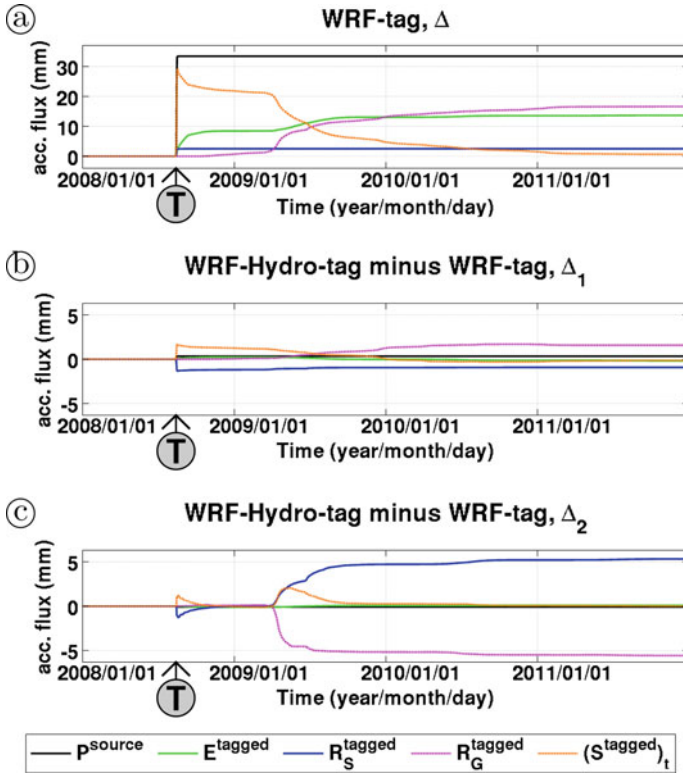


**Fig. 3** **a** Daily time series of the tagged terrestrial water fluxes from the budget Eq. 1 derived from WRF-tag, spatially averaged in the study region  $\Delta$  and displayed as daily accumulated sums [mm] from 1 January 2008 to 31 December 2011. **b** As in (a), except for the difference between WRF-Hydro-tag and WRF-tag spatially averaged in the subregion  $\Delta_1$ . **c** As in (a), except for the difference between WRF-Hydro-tag and WRF-tag spatially averaged in the subregion  $\Delta_2$

(see Fig. 3b) is slightly depleted by  $E^{tagged}$  during 2008. During 2009 and 2010, this excess of tagged soil moisture is mostly depleted by  $R_G^{tagged}$ , and to a much lower extend by  $R_S^{tagged}$  as well. The fact that the tagged subsurface lateral water flow in WRF-Hydro-tag accelerates the deep infiltration of tagged soil moisture in  $\Delta_1$  induces a relatively smaller  $\Delta_1$ -average tagged soil moisture amount from 2010. This can be related to Sprenger et al. [4] who showed that the travel time of precipitated water in the root zone is mainly driven by subsequent precipitation amounts. Our result further shows that the lateral subsurface flow contributes to accelerate this washing out of precipitated water in moderate topography areas. In  $\Delta_2$ , the excess of tagged soil moisture in WRF-Hydro-tag (see Fig. 3c) is mostly depleted by  $R_S^{tagged}$  during the few weeks following the tagging event. From 2009, the delayed production of  $R_S^{tagged}$  in WRF-Hydro-tag is mostly counterbalanced by a reduction of  $R_G^{tagged}$ .

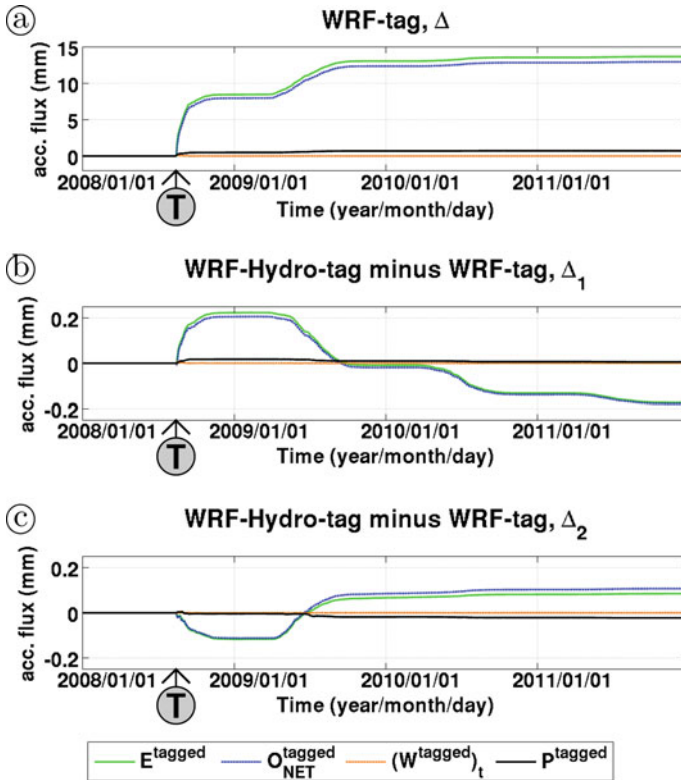


**Fig. 4** a Daily time series of the tagged atmospheric water fluxes from the budget Eq. 2 derived from WRF-tag, spatially averaged in the study region  $\Delta$  and displayed as daily accumulated sums [mm] from 1 January 2008 to 31 December 2011. b As in (a), except for the difference between WRF-Hydro-tag and WRF-tag spatially averaged in the subregion  $\Delta_1$ . c As in (a), except for the difference between WRF-Hydro-tag and WRF-tag spatially averaged in the subregion  $\Delta_2$

The tagged ponded water infiltration in WRF-Hydro-tag enhances  $E^{tagged}$  during the tagging period and the following weeks, especially in  $\Delta_1$  as shown in Fig. 4b. In the case of  $\Delta_2$ ,  $E^{tagged}$  is rather reduced in association with the exfiltration of tagged soil moisture towards the surface, as shown in Fig. 4c. Accordingly,  $\Delta_1$ -average  $P^{tagged}$  is slightly enhanced, whereas  $\Delta_2$ -average  $P^{tagged}$  remains almost unchanged during the tagging period and the following weeks.

During the warm months of 2009, 2010 and 2011,  $E^{tagged}$  in  $\Delta_1$  is generally lower in WRF-Hydro-tag than in WRF-tag, in relation with a faster deep infiltration of the tagged soil moisture in WRF-Hydro-tag. In  $\Delta_2$ , this enhanced tagged infiltration is overbalanced by the tagged exfiltration which maintains some tagged soil moisture in the upper soil layers and enhances  $E^{tagged}$ . As  $\Delta_2$  is much smaller than  $\Delta_1$ , the increase of  $\Delta_2$ -average  $E^{tagged}$  in 2009 underbalances the decrease of  $\Delta_1$ -average

$E^{tagged}$ , so that both  $\Delta_1$ -average  $P^{tagged}$  and  $\Delta_2$ -average  $P^{tagged}$  decrease from 2009 as shown in Fig. 4b and c.

In summary for the case of the upper Danube river basin, the consideration of the fate of ponded water in WRF-Hydro-tag primarily enhances the tagged infiltration, thereby increasing the transit time of the precipitated water during the few weeks following the tagging event, which slightly increases the tagged evaporation and very slightly increases the tagged precipitation. This primary effect is however reduced in steep topography gradient areas where the enhanced tagged exfiltration counterbalances the enhanced tagged infiltration. Secondly, after a few months the subsurface lateral water flow in WRF-Hydro-tag induces a faster deep infiltration of the tagged soil moisture in low topography gradient areas, thereby decreasing the root zone transit time of the precipitated water, which slightly decreases the tagged surface evaporation and very slightly decreases the tagged precipitation.

## References

1. J. Arnault, J. Wei, T. Rummeler, B. Fersch, Z. Zhang, G. Jung, S. Wagner, H. Kunstmann, A joint soil-vegetation-atmospheric water tagging procedure with WRF-Hydro: Implementation and application to the case of precipitation partitioning in the upper Danube river basin. *Water Resour. Res.* **55**, 6217–6243 (2019)
2. D.J. Gochis, W. Yu, D.N. Yates, The WRF-Hydro model technical description and user's guide, version 3.0, NCAR Technical Document, 120 p (2015), [http://www.ral.ucar.edu/projects/wrf\\_hydro/](http://www.ral.ucar.edu/projects/wrf_hydro/)
3. W.C. Skamarock, J.B. Klemp, A time-split nonhydrostatic atmospheric model for weather research and forecasting applications. *J. Comp. Phys.* **227**, 3465–3485 (2008)
4. M. Sprenger, S. Seeger, T. Blume, M. Weiler, Travel times in the vadose zone: Variability in space and time. *Water Resour. Res.* **52**, 5727–5754 (2016)